INTERNATIONAL JOURNAL FOR NUMERICAL METHODS IN FLUIDS
Int. J. Numer. Meth. Fluids 2010; **63**:374–394
Published online 16 June 2009 in Wiley InterScience (www.interscience.wiley.com). DOI: 10.1002/fld.2081

Slip effects on the peristaltic flow of a Jeffrey fluid in an asymmetric channel under the effect of induced magnetic field

S. Nadeem*,† and Safia Akram

Department of Mathematics, Quaid-i-Azam University 45320, Islamabad 44000, Pakistan

SUMMARY

In the present study, we investigated the effects of slip and induced magnetic field on the peristaltic flow of a Jeffrey fluid in an asymmetric channel. The governing two-dimensional equations for momentum, magnetic force function and energy are simplified by using the assumptions of long wavelength and low but finite Reynolds number. The reduced problem has been solved by Adomian decomposition method (ADM) and closed form solutions have been presented. Further, the exact solution of the proposed problem has also been computed and the mathematical comparison shows that both solutions are almost similar. The effects of pertinent parameters on the pressure rise per wavelength are investigated using numerical integration. The expressions for pressure rise, friction force, velocity, temperature, magnetic force function and the stream lines against various physical parameters of interest are shown graphically. Moreover, the behavior of different kinds of wave shape are also discussed. Copyright © 2009 John Wiley & Sons, Ltd.

Received 20 November 2008; Revised 19 March 2009; Accepted 6 April 2009

KEY WORDS: Adomian decomposition method; exact solution; Jeffrey fluid; heat transfer; partial slip; induced magnetic field; peristaltic motion

1. INTRODUCTION

A flow phenomena in which the fluid velocity indirectly contacts with a solid boundary having the same velocity as the boundary itself is known as no slip condition. However, in some situations, such as fluid flow past a permeable walls [1], slotted plates [2], rough and coated surfaces [3], emulsion, suspensions, foam, polymer solutions, gas and liquid flow in microdevices [4], the traditional no slip condition does not hold valid and should be replaced by a partial slip boundary condition. The slip boundary condition was first discussed by Navier [5], in which the velocity is proportional to the shear stress at the boundary. After the initiation of Navier, a number of researchers have discussed the partial slip boundary condition for different kinds of fluids with different geometries [6–9].

*Correspondence to: S. Nadeem, Department of Mathematics, Quaid-i-Azam University 45320, Islamabad 44000, Pakistan.
†E-mail: snqau@hotmail.com

Peristaltic pumping is a form of fluid transport that occurs when a progressive wave of area contraction or expansion propagates along the length of a distensible tube containing the fluid. Peristaltic flow occurs widely in urine transport from kidney to bladder, swallowing food through the esophagus, movement of chyme in the gastrointestinal tract, transport of spermatozoa in the ducts efferentes of the male reproductive tract, movement of ovum in the female fallopian tubes, vasomotion of small blood vessels, transport of slurries, corrosive fluids, sanitary fluids and noxious fluids in nuclear industry. Considering these applications, a number of studies have been carried out, which involve Newtonian and non-Newtonian fluids with different kinds of geometries [10–24].

The effects of MHD on the peristaltic flow problems have applications in physiological fluids such as blood flow, blood pump machines and for theoretical research on the operation of peristaltic MHD compressor. Further, the application of magnetic field occurs in the form of a device, magnetic resonance imaging (MRI), which is used for diagnosis of brain, vascular diseases and all the human body. Only a limited attention has been focused to such a kind of study in peristalsis [25–27].

Considering these importances, the aim of the present investigation is to discuss the effects of induced magnetic field on the peristaltic flow of a Jeffrey fluid in an asymmetric channel in the presence of partial slip condition. The governing equations of motion, magnetic force function and energy in the presence of dissipation terms are simplified by long wavelength and low but finite Reynolds number. The simplified equations are then solved by Adomian decomposition method (ADM) and exact solutions are also calculated. It is found that the ADM solutions and exact solutions are almost the same. The graphical results are also presented to gauge the effects of certain physical parameters. Finally, the trapping phenomena for different wave shapes have also been discussed pictorically.

2. MATHEMATICAL FORMULATION

Let us consider the peristaltic flow of an incompressible, electrically conducting non-Newtonian fluid (Jeffrey fluid) in a two-dimensional channel of width d_1+d_2. The lower wall of the channel is maintained at temperature T_1, whereas the upper wall has temperature T_0. The flow is generated by sinusoidal wave trains propagating with constant speed c along the channel walls. We considered a rectangular coordinate system for the channel in which the X-axis is taken along the centerline of the channel and the Y-axis is transverse to it. An external transverse uniform constant magnetic field, H_0, induced magnetic field, $H(h_X(X,Y,t), H_0+h_Y(X,Y,t), 0)$ and the total magnetic field, $H^+(h_X(X,Y,t), H_0+h_Y(X,Y,t), 0)$, are taken into account. Finally, the channel walls are considered to be non-conductive and the geometry of the wall surface is defined as

$$Y=H_1=d_1+a_1\mathrm{Cos}\left[\frac{2\pi}{\lambda}(X-ct)\right], \quad Y=H_2=-d_2-b_1\mathrm{Cos}\left[\frac{2\pi}{\lambda}(X-ct)+\phi\right] \tag{1}$$

where a_1 and b_1 are the amplitudes of the waves, λ is the wavelength, d_1+d_2 is the width of the channel, c is the velocity of propagation, t is the time and X is the direction of wave propagation, the phase difference ϕ varies in the range $0\leqslant\phi\leqslant\pi$, $\phi=0$ corresponding to symmetric channel with waves out of phase and $\phi=\pi$ the waves are in phase, and further a_1, b_1, d_1, d_2 and ϕ satisfies the condition

$$a_1^2+b_1^2+2a_1b_1\cos\phi\leqslant(d_1+d_2)^2$$

DOI: 10.1002/fld

The equations that govern the MHD flow of a Jeffrey fluid are given as

(i) Maxwell's equation

$$\nabla\cdot\mathbf{H}=0,\quad \nabla\cdot\mathbf{E}=\mathbf{0} \tag{2}$$

$$\nabla\wedge\mathbf{H}=\mathbf{J},\quad \mathbf{J}=\boldsymbol{\sigma}\{\mathbf{E}+\boldsymbol{\mu}_e(\mathbf{V}\wedge\mathbf{H})\} \tag{3}$$

$$\nabla\wedge\mathbf{E}=-\boldsymbol{\mu}_e\frac{\partial\mathbf{H}}{\partial\mathbf{t}} \tag{4}$$

(ii) The continuity equation

$$\nabla\cdot\mathbf{V}=0 \tag{5}$$

(iii) The equations of motion

$$\rho\left(\frac{\partial\mathbf{V}}{\partial t}+(\mathbf{V}\cdot\nabla)\mathbf{V}\right)=\operatorname{div}\mathbf{T}-\nabla\left(\frac{1}{2}\boldsymbol{\mu}_e(\mathbf{H}^+)^2\right)-\boldsymbol{\mu}_e(\mathbf{H}^+\cdot\nabla)\mathbf{H}^+ \tag{6}$$

where

$$\mathbf{T}=-\mathbf{pI}+S$$

In which for the extra stress tensor $\mathbf{S}$ for Jeffrey fluid is defined as

$$\mathbf{S}=\frac{\mu}{1+\lambda_1}(\dot{\gamma}+\lambda_2\ddot{\gamma})$$

(iv) The energy equation

$$\rho\frac{\mathrm{d}\mathbf{e}}{\mathrm{d}t}=\boldsymbol{\tau}\cdot\mathbf{L}-\mathbf{div}\,\mathbf{q}+\boldsymbol{\rho}\mathbf{r} \tag{7}$$

In the above equations, $\mathbf{V}$ is the velocity vector, μ is the viscosity of the fluid, p is the pressure, $\mathbf{E}$ is an induced electric field, $\mathbf{J}$ is the current density, $\boldsymbol{\mu}_e$ is the magnetic permeability, σ is the electric conductivity, λ_1 is the ratio of relaxation to retardation times, $\dot{\gamma}$ is the shear rate, λ_2 the retardation time and dots denote differentiation with respect to time, $\mathbf{q}=(-K'\operatorname{div}\mathbf{T}, K'$ being the thermal conductivity) is the heat flux vector, $\mathbf{r}$ is the internal heat generation (radial heating) taken here to be zero, and $e=C'\mathbf{T}, C'$ being specific heat is the specific internal energy.

Combining Equations (2) and (3)–(5), we obtain the induction equation as follows:

$$\frac{\partial\mathbf{H}^+}{\partial t}=\nabla\wedge(\mathbf{V}\wedge\mathbf{H}^+)+\frac{1}{\xi}\nabla^2\mathbf{H}^+ \tag{8}$$

where $\xi=1/\sigma\boldsymbol{\mu}_e$ is the magnetic diffusively.

Introducing a wave frame (x, y) moving with velocity c away from the fixed frame (X, Y) by the transformation

$$x=X-ct,\quad y=Y,\quad u=U-c,\quad v=V$$

DOI: 10.1002/fld

Defining

$$\bar{x}=\frac{x}{\lambda},\ \bar{y}=\frac{y}{d_1},\ \bar{u}=\frac{u}{c},\ \bar{v}=\frac{v}{c},\ \delta=\frac{d_1}{\lambda},\ d=\frac{d_2}{d_1},\ \bar{p}=\frac{d_1^2 p}{\mu c\lambda},\ \bar{t}=\frac{ct}{\lambda},\ h_1=\frac{H_1}{d_1},\ h_2=\frac{H_2}{d_2},\ a=\frac{a_1}{d_1}$$

$$b=\frac{b_1}{d_1},\ Re=\frac{cd_1}{\nu},\ \bar{\Psi}=\frac{\Psi}{cd_1},\ \bar{\Phi}=\frac{\Phi}{H_0 d_1},\ p_m=p+\frac{1}{2}Re\,\delta\frac{\boldsymbol{\mu}_e(H^+)^2}{\rho c^2},\ Nu=\frac{q_w d_1}{K'(T_1-T_0)}$$

$$R_m=\sigma\boldsymbol{\mu}_e d_1 c,\ S_1=\frac{H_0}{c}\sqrt{\frac{\boldsymbol{\mu}_e}{\rho}},\ \theta=\frac{T-T_0}{T_1-T_0},\ E_c=\frac{c^2}{C'(T_1-T_0)},\ Pr=\frac{\rho\nu C'}{K'},\ \bar{S}=\frac{Sd_1}{\mu c}$$

Using the above non-dimensional quantities, the equations that govern the MHD flow in terms of the stream function $\Psi(x,y)$ and magnetic force function $\Phi(x,y)$ (dropping the bars and using $u=\partial\Psi/\partial y, v=-\delta(\partial\Psi/\partial x), h_x=\partial\Phi/\partial y, h_y=-\delta\partial\Phi/\partial x$) are

$$Re\,\delta(\Psi_y\Psi_{xy}-\Psi_x\Psi_{yy})=-\frac{\partial p_m}{\partial x}+\delta\frac{\partial}{\partial x}(S_{xx})+\frac{\partial}{\partial y}(S_{xy})$$
$$+Re\,S_1^2\Phi_{yy}+Re\,S_1^2\delta(\Phi_y\Phi_{xy}-\Phi_x\Phi_{yy}) \tag{9}$$

$$Re\,\delta^3(\Psi_x\Psi_{xy}-\Psi_y\Psi_{xx})=-\frac{\partial p_m}{\partial y}+\delta^2\frac{\partial}{\partial x}(S_{yx})+\delta\frac{\partial}{\partial y}(S_{yy})$$
$$-Re\,\delta^2 S_1^2\Phi_{xy}-Re\,S_1^2\delta^3(\Phi_y\Phi_{xx}-\Phi_x\Phi_{xy}) \tag{10}$$

$$Re\,\delta(\Psi_y\theta_x-\Psi_x\theta_y)=\frac{1}{Pr}(\theta_{yy}+\delta^2\theta_{xx})$$
$$+\frac{E_c}{(1+\lambda_1)}\left(1+\frac{\lambda_2 c\delta}{d_1}\left(\Psi_y\frac{\partial}{\partial x}-\Psi_x\frac{\partial}{\partial y}\right)\right)$$
$$\times(4\delta^2\Psi_{xy}^2+(\Psi_{yy}-\delta^2\Psi_{xx})^2) \tag{11}$$

$$\Psi_y-\delta(\Psi_y\Phi_x-\Psi_x\Phi_y)+\frac{1}{R_{\mathrm{m}}}(\Phi_{yy}+\delta^2\Phi_{xx})=E \tag{12}$$

where

$$S_{xx}=\frac{2\delta}{1+\lambda_1}\left(1+\frac{\lambda_2 c\delta}{d_1}\left(\Psi_y\frac{\partial}{\partial x}-\Psi_x\frac{\partial}{\partial y}\right)\right)\Psi_{xy}$$

$$S_{xy}=\frac{1}{1+\lambda_1}\left(1+\frac{\lambda_2 c\delta}{d_1}\left(\Psi_y\frac{\partial}{\partial x}-\Psi_x\frac{\partial}{\partial y}\right)\right)(\Psi_{yy}-\delta^2\Psi_{xx})$$

$$S_{yy}=-\frac{2\delta}{1+\lambda_1}\left(1+\frac{\lambda_2 c\delta}{d_1}\left(\Psi_y\frac{\partial}{\partial x}-\Psi_x\frac{\partial}{\partial y}\right)\right)\Psi_{xy}$$

DOI: 10.1002/fld

The corresponding boundary conditions are

$$\Psi = \frac{q}{2} \quad \text{at} \quad y = h_1 = 1 + a\cos 2\pi x$$

$$\Psi = -\frac{q}{2} \quad \text{at} \quad y = h_2 = -d - b\cos(2\pi x + \phi)$$

$$\frac{\partial \Psi}{\partial y} + \frac{\beta}{(1+\lambda_1)}\frac{\partial^2 \Psi}{\partial y^2} = -1 \quad \text{at} \quad y = h_1$$

$$\frac{\partial \Psi}{\partial y} - \frac{\beta}{(1+\lambda_1)}\frac{\partial^2 \Psi}{\partial y^2} = -1 \quad \text{at} \quad y = h_2 \tag{13}$$

$$\theta = 0 \quad \text{at} \quad y = h_1$$

$$\theta = 1 \quad \text{at} \quad y = h_2 \tag{14}$$

$$\Phi = 0 \quad \text{at} \quad y = h_1 \quad \text{and} \quad y = h_2 \tag{15}$$

where q is the flux in the wave frame, β is the slip parameter a, b, ϕ and d satisfy the relation

$$a^2 + b^2 + 2ab\cos\phi \leqslant (1+d)^2$$

Under the assumption of long wavelength $\delta \ll 1$ and low but finite Reynolds number neglecting the terms of order δ and higher, Equations (9)–(12) take the form

$$-\frac{\partial p}{\partial x} + \frac{\partial}{\partial y}\left(\frac{1}{1+\lambda_1}\frac{\partial^2 \Psi}{\partial y^2}\right) + ReS_1^2 \Phi_{yy} = 0 \tag{16}$$

$$-\frac{\partial p}{\partial y} = 0 \tag{17}$$

$$\frac{1}{Pr}\theta_{yy} + \frac{E_c}{(1+\lambda_1)}\Psi_{yy}^2 = 0 \tag{18}$$

$$\Phi_{yy} = R_{\mathrm{m}}\left(E - \frac{\partial \Psi}{\partial y}\right) \tag{19}$$

Elimination of pressure from Equations (16) and (17) yields

$$\frac{\partial^2}{\partial y^2}\left(\frac{1}{1+\lambda_1}\frac{\partial^2 \Psi}{\partial y^2}\right) + ReS_1^2 \Phi_{yyy} = 0 \tag{20}$$

$$\frac{1}{Pr}\theta_{yy} + \frac{E_c}{(1+\lambda_1)}\Psi_{yy}^2 = 0 \tag{21}$$

$$\Phi_{yy} = R_{\mathrm{m}}\left(E - \frac{\partial \Psi}{\partial y}\right) \tag{22}$$

DOI: 10.1002/fld

With the help of Equation (22), Equation (20) takes the form

$$\frac{\partial^3 \Psi}{\partial y^3} + M^2(1+\lambda_1)\left(E - \frac{\partial \Psi}{\partial y}\right) = F_3 \tag{23}$$

where F_3 is a constant, $M^2 = R_m Re S_1^2$, Re is the Reynolds number, S_1 is the Strommer's number (magnetic force number) and R_m is the magnetic Reynolds number.

3. METHODS OF SOLUTION

3.1. Exact solution

The exact solution of Equation (23) can be written as

$$\Psi = F_0 + F_1 \cosh(m_1 y) + F_2 \sinh(m_1 y) + Ey - \frac{F_3}{m_1^2} y \tag{24}$$

where

$$m_1 = M\sqrt{(1+\lambda_1)}$$

and F_0, F_1, F_2 and F_3 are functions of x only and can be calculated using boundary conditions (13)

$$\begin{aligned}
F_0 &= \frac{q m_1 (h_2+h_1) + \begin{pmatrix} 2(h_2+h_1) + \\ q m_1^2 \dfrac{\beta}{(1+\lambda_1)}(h_2+h_1) \end{pmatrix} \tanh\left[m_1\left(\frac{h_1-h_2}{2}\right)\right]}{2(h_2-h_1)m_1 + 2\left(2 + m_1^2 \dfrac{\beta}{(1+\lambda_1)}(h_2-h_1)\right)\tanh\left[m_1\left(\frac{h_1-h_2}{2}\right)\right]} \\
F_1 &= \frac{(q+h_1-h_2)\,\mathrm{sech}\left[m_1\left(\dfrac{h_1-h_2}{2}\right)\right]\sinh\left[m_1\left(\dfrac{h_1+h_2}{2}\right)\right]}{(h_1-h_2)m_1 - \left(2 + m_1^2 \dfrac{\beta}{(1+\lambda_1)}(h_2-h_1)\right)\tanh\left[m_1\left(\dfrac{h_1-h_2}{2}\right)\right]} \\
F_2 &= \frac{(q+h_1-h_2)\,\mathrm{sech}\left[m_1\left(\dfrac{h_1-h_2}{2}\right)\right]\cosh\left[m_1\left(\dfrac{h_1+h_2}{2}\right)\right]}{(h_2-h_1)m_1 + \left(2 + m_1^2 \dfrac{\beta}{(1+\lambda_1)}(h_2-h_1)\right)\tanh\left[m_1\left(\dfrac{h_1-h_2}{2}\right)\right]} \\
F_3 &= \frac{\begin{matrix} m_1^3(q - h_1 E + E h_2) + \\ \left(2m_1^2(E+1) + m_1^4(q - h_1 E + E h_2)\dfrac{\beta}{(1+\lambda_1)}\right)\tanh\left[m_1\left(\dfrac{h_1-h_2}{2}\right)\right] \end{matrix}}{\begin{matrix} (h_2-h_1)m_1 + \left(2 + m_1^2 \dfrac{\beta}{(1+\lambda_1)}(h_2-h_1)\right)\tanh\left[m_1\left(\dfrac{h_1-h_2}{2}\right)\right] \\ m_1^3(q - h_1 E + E h_2) + \end{matrix}}
\end{aligned} \tag{25}$$

DOI: 10.1002/fld

3.2. Solution by the ADM

According to ADM, we rewrite Equation (23) in the operator form as

$$L_{yyy}\Psi=(F_3-m_1^2E)+m_1^2\Psi_y \tag{26}$$

Applying the inverse operator $L_{yyy}^{-1}=\int\int\int[.]\,dy\,dy\,dy$, we can write Equation (26) as

$$\Psi=A+By+C\frac{y^2}{2!}+(F_3-m_1^2E)\frac{y^3}{3!}+m_1^2L_{yyy}^{-1}(\Psi_y) \tag{27}$$

where

$$m_1^2=M^2(1+\lambda_1)$$

and A, B, C, F_3 are functions of x. Now we decompose Ψ as

$$\Psi=\sum_{n=0}^{\infty}\Psi_n \tag{28}$$

Substituting Ψ into Equation (27), we obtain

$$\begin{aligned}\Psi_0&=A+By+C\frac{y^2}{2!}+(F_3-m_1^2E)\frac{y^3}{3!}\\ \Psi_{n+1}&=m_1^2\int\int\int(\Psi_n)_y\,dy\,dy\,dy,\quad n\geqslant 0\end{aligned} \tag{29}$$

Therefore,

$$\begin{aligned}\Psi_1&=m_1^2\left(B\frac{y^3}{3!}+C\frac{y^4}{4!}+(F_3-m_1^2E)\frac{y^5}{5!}\right)\\ \Psi_2&=m_1^4\left(B\frac{y^5}{5!}+C\frac{y^6}{6!}+(F_3-m_1^2E)\frac{y^7}{7!}\right)\\ &\vdots\\ \Psi_n&=m_1^{2n}\left(B\frac{y^{2n+1}}{(2n+1)!}+C\frac{y^{2n+2}}{(2n+2)!}+(F_3-m_1^2E)\frac{y^{2n+3}}{(2n+3)!}\right),\quad n>0\end{aligned} \tag{30}$$

According to (28), the closed form of Ψ can be written as

$$\Psi=A+\sinh(m_1y)\left(\frac{B}{m_1}+\frac{1}{m_1^3}(F_3-m_1^2E)\right)+\frac{C}{m_1^2}(\cosh(m_1y)-1)-\frac{1}{m_1^2}(F_3-m_1^2E)y$$

which can be put in the simplest form

$$\Psi=F_0+F_1\cosh(m_1y)+F_2\sinh(m_1y)+Ey-\frac{F_3}{m_1^2}y \tag{31}$$

Now the Adomian solution (31) and exact solution (24) are exactly the same in which $F_i(i=0\text{–}3)$ are calculated using boundary conditions that are defined in Equation (25).

DOI: 10.1002/fld

Making use of Equation (24), the exact solution of Equation (21) satisfying the boundary condition (14) can be written as

$$\theta=-\frac{E_c Pr}{(1+\lambda_1)}\begin{pmatrix}\frac{F_1^2}{2}m_1^4Y^2+\frac{1}{8}(F_1^2+F_2^2)m_1^2\cosh 2(m_1Y)-\frac{1}{4}(F_1^2+F_2^2)m_1^4Y^2\\ \frac{1}{4}F_1F_2m_1^2\sinh 2(m_1Y)\end{pmatrix}+c_1Y+c_2 \quad (32)$$

where

$$c_1=\frac{-1}{(h_1-h_2)}$$
$$+\frac{E_c Pr}{(1+\lambda_1)(h_1-h_2)}\begin{pmatrix}\frac{1}{2}F_1^2m_1^4(h_1^2-h_2^2)+\frac{1}{4}(F_1^2+F_2^2)m_1^4(h_1^2-h_2^2)\\ +\frac{1}{8}(F_1^2+F_2^2)m_1^2(\cosh 2(m_1h_1)-\cosh 2(m_1h_2))\\ +\frac{1}{4}F_1F_2m_1^2(\sinh 2(m_1h_1)-\sinh 2(m_1h_2))\end{pmatrix}$$
$$c_2=\frac{E_c Pr}{(1+\lambda_1)}\begin{pmatrix}\frac{1}{2}F_1^2m_1^4h_1^2+\frac{1}{4}F_1F_2m_1^2\sinh 2(m_1h_1)\\ +\frac{1}{8}(F_1^2+F_2^2)m_1^2\cosh 2(m_1h_1)-\frac{1}{4}(F_1^2+F_2^2)m_1^4h_1^2\end{pmatrix}-c_1h_1$$

The exact solution of Equation (22) is defined as

$$\Phi=c_3y+c_4+\frac{F_3R_m}{m_1^2}\frac{y^2}{2}-R_m\left(\frac{F_1}{m_1}\sinh(m_1y)+\frac{F_2}{m_1}\cosh(m_1y)\right) \quad (33)$$

where c_3 and c_4 are calculated using boundary condition (15) and are

$$c_3=\frac{R_m}{2}(h_1+h_2)\begin{pmatrix}m_1(q-h_1E+Eh_2)+\left(\begin{array}{c}2(E+1)+\\ \frac{\beta}{(1+\lambda_1)}m_1^2(q-h_1E+Eh_2)\end{array}\right)\tanh\left[m_1\left(\frac{h_1-h_2}{2}\right)\right]\\ \hline (h_1-h_2)m_1-\left(2+m_1^2\frac{\beta}{(1+\lambda_1)}(h_2-h_1)\right)\tanh\left[m_1\left(\frac{h_1-h_2}{2}\right)\right]\end{pmatrix}$$

$$c_4=\frac{R_m}{m_1}\begin{pmatrix}2(q+h_1-h_2)+m_1^2h_1h_2(q-h_1E+Eh_2)\\ +m_1h_1h_2\left(2(E+1)+\frac{\beta}{(1+\lambda_1)}m_1^2(q-h_1E+Eh_2)\right)\tanh\left[m_1\left(\frac{h_1-h_2}{2}\right)\right]\\ \hline 2(h_2-h_1)m_1+2\left(2+m_1^2\frac{\beta}{(1+\lambda_1)}(h_2-h_1)\right)\tanh\left[m_1\left(\frac{h_1-h_2}{2}\right)\right]\end{pmatrix}$$

DOI: 10.1002/fld

The expression for axial induced magnetic field can be obtained with the help of $h_x = \partial\Phi/\partial y$, which are as follows:

$$h_x(x,y) = \frac{R_m \left(\begin{array}{c} 2(q+h_1-h_2)\,\mathrm{sech}\left[m_1\left(\frac{h_1-h_2}{2}\right)\right]\sinh\left[m_1\left(\frac{h_1+h_2}{2}-y\right)\right]+ \\ \left(\begin{array}{c} m_1(q-h_1E+h_2E)+ \\ \left(2(E+1)+\frac{\beta}{(1+\lambda_1)}m_1^2(q-h_1E+h_2E)\right)\tanh\left[m_1\left(\frac{h_1-h_2}{2}\right)\right] \end{array} \right)(2y-h_1-h_2) \end{array} \right)}{2(h_2-h_1)m_1+2\left(2+m_1^2\frac{\beta}{(1+\lambda_1)}(h_2-h_1)\right)\tanh\left[m_1\left(\frac{h_1-h_2}{2}\right)\right]} \tag{34}$$

where $\lambda_1 \to 0$ and $M \to 0$ the solutions of Misra can be recovered as a special case of our problem. Moreover, the Jeffrey problem with induced magnetic field has not been discussed so far.

The flux at any axial station in the fixed frame is

$$\bar{Q} = \int_{h2}^{h1}(u+1)\,\mathrm{d}y = \int_{h2}^{h1} u\,\mathrm{d}y + \int_{h2}^{h1}\mathrm{d}y = q+h_1-h_2$$

The average volume flow rate over one period ($T = \lambda/c$) of the peristaltic wave is defined as

$$Q = \frac{1}{T}\int_0^T \bar{Q}\,\mathrm{d}t = \frac{1}{T}\int_0^T (q+h_1-h_2)\,\mathrm{d}t = q+1+d \tag{35}$$

The pressure gradient is obtained from the dimensionless momentum equation for the axial velocity

$$\frac{\mathrm{d}p}{\mathrm{d}x} = \frac{1}{(1+\lambda_1)}\Psi_{yyy} + M^2(E-\Psi_y) \tag{36}$$

Substituting the value of Ψ given in (24), Equation (36) takes the form

$$\frac{\mathrm{d}p}{\mathrm{d}x} = \frac{m_1^3(q-h_1E+h_2E)+\left(2m_1^2(E+1)+\frac{\beta}{(1+\lambda_1)}m_1^4(q-h_1E+h_2E)\right)\tanh\left[m_1\left(\frac{h_1-h_2}{2}\right)\right]}{(1+\lambda_1)\left((h_2-h_1)m_1+\left(2+m_1^2\frac{\beta}{(1+\lambda_1)}(h_2-h_1)\right)\tanh\left[m_1\left(\frac{h_1-h_2}{2}\right)\right]\right)} \tag{37}$$

For one wavelength the integration of Equation (37) yields

$$\Delta p = \int_0^1 \frac{\mathrm{d}p}{\mathrm{d}x}\,\mathrm{d}x \tag{38}$$

The expression for frictional force is defined as

$$F = \int_0^1 \frac{\mathrm{d}p}{\mathrm{d}x}\,\mathrm{d}x \tag{39}$$

where the expression for $\mathrm{d}p/\mathrm{d}x$ is defined in Equation (37).

DOI: 10.1002/fld

The axial velocity component in fixed frame is calculated as

$$U(X,Y,t)=1+\Psi_y$$

$$m_1(h_1-h_2+q)\left(\begin{array}{c}-1+\operatorname{sech}\left[m_1\left(\dfrac{h_1-h_2}{2}\right)\right]\\ \cosh\left[m_1\left(\dfrac{h_1+h_2}{2}-Y\right)\right]\end{array}\right)$$

$$=\frac{+m_1^2\dfrac{\beta}{(1+\lambda_1)}(h_2-h_1-q+Eh_2)\tanh\left[m_1\left(\dfrac{h_1-h_2}{2}\right)\right]}{(h_2-h_1)m_1+\left(2+m_1^2\dfrac{\beta}{(1+\lambda_1)}(h_2-h_1)\right)\tanh\left[m_1\left(\dfrac{h_1-h_2}{2}\right)\right]} \tag{40}$$

where

$$h_1=1+a\cos[2\pi(X-t)] \quad \text{and} \quad h_2=-d-b\cos[2\pi(X-t)+\phi]$$

The expression for the Nusselt number for the upper wall is defined as

$$Nu=-\left.\frac{\partial\theta}{\partial y}\right|_{y=h_1}$$

Similarly, we calculate for the lower wall.

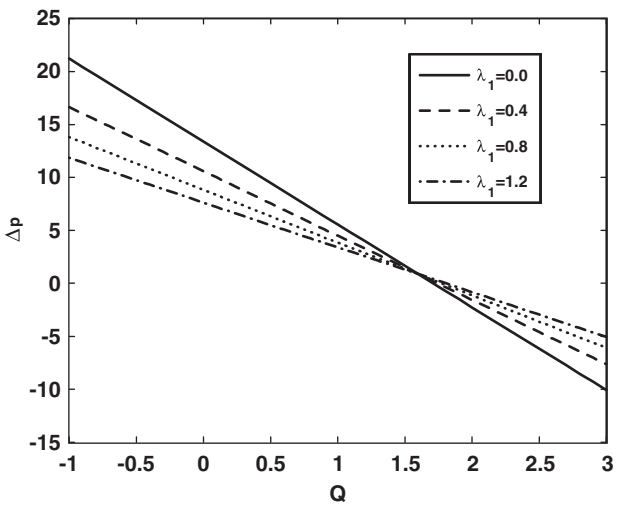

Figure 1. Variation of Δp with Q for different values of λ_1 at $a=0.7, b=1.2$, $d=1.4, E=4, M=0.5, \phi=\pi/6, \beta=0.04$ (sinusoidal wave).

DOI: 10.1002/fld

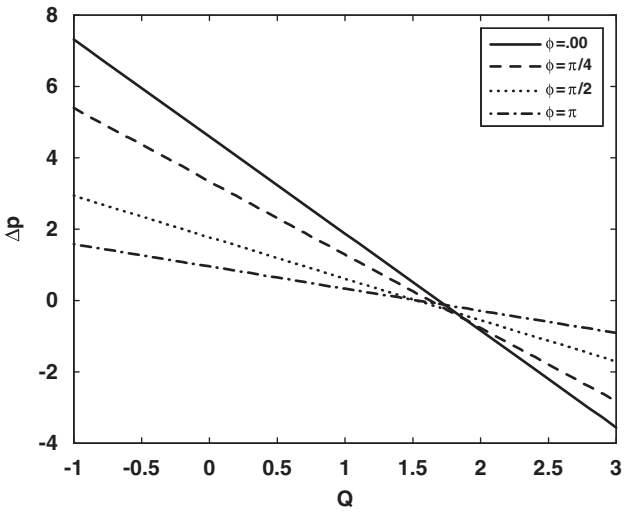

Figure 2. Variation of Δp with Q for different values of ϕ at $a=0.7, b=1.2$, $d=1.5, E=4, M=1.5, \lambda_1=0.5, \beta=0.04$ (sinusoidal wave).

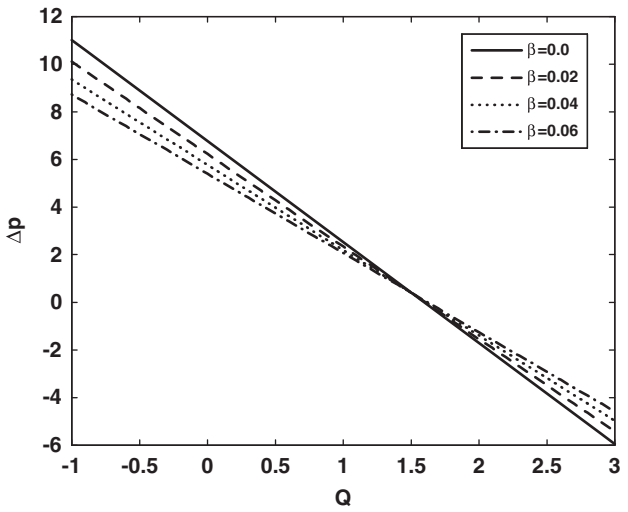

Figure 3. Variation of Δp with Q for different values of β at $a=0.7$, $b=1.2, d=1.4, E=4, M=0.5, \lambda_1=0.5, \phi=\pi/6$ (sinusoidal wave).

4. EXPRESSIONS FOR DIFFERENT WAVE SHAPES

The non-dimensional expressions for three considered wave form are given by the following [15]

1. Sinusoidal wave:

$$h(x)=1+\phi\sin(2\pi x)$$

DOI: 10.1002/fld

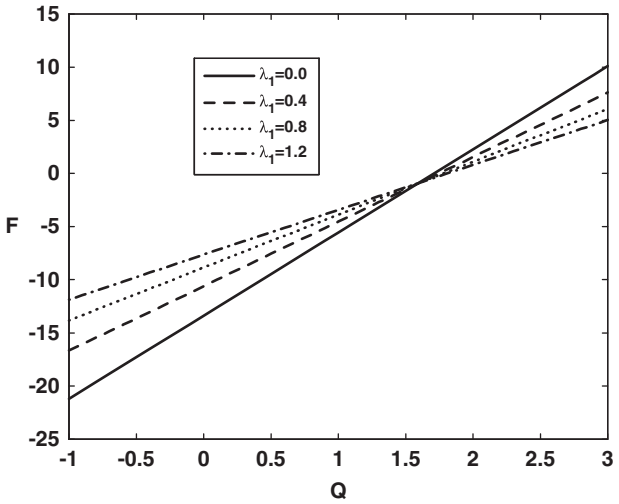

Figure 4. Variation of F with Q for different values of λ_1 at $a=0.7, b=1.2$, $d=1.4, E=4, M=0.5, \phi=\pi/6, \beta=0.04$ (sinusoidal wave).

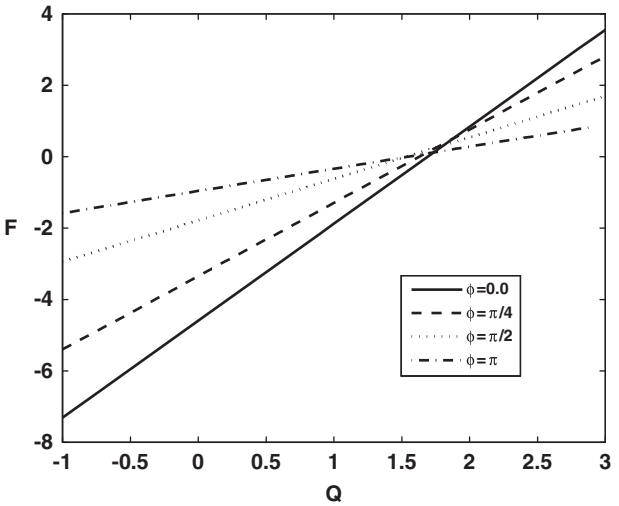

Figure 5. Variation of F with Q for different values of ϕ at $a=0.7, b=1.2$, $d=1.5, E=4, M=1.5, \lambda_1=0.5, \beta=0.04$ (sinusoidal wave).

2. Triangular wave:

$$h(x)=1+\phi\left[\frac{8}{\pi^3}\sum_{m=1}^{\infty}\frac{(-1)^{m+1}}{(2m-1)^2}\sin(2\pi(2m-1)x)\right]$$

DOI: 10.1002/fld

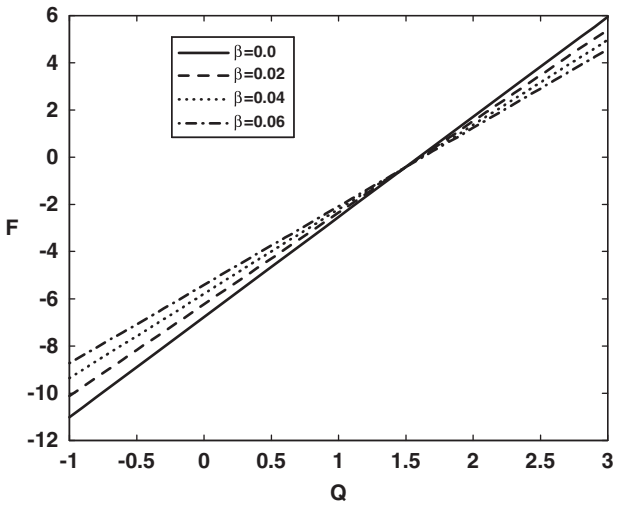

Figure 6. Variation of F with Q for different values of β at $a=0.7, b=1.2$, $d=1.4, E=4, M=0.5, \lambda_1=0.5, \phi=\pi/6$ (sinusoidal wave).

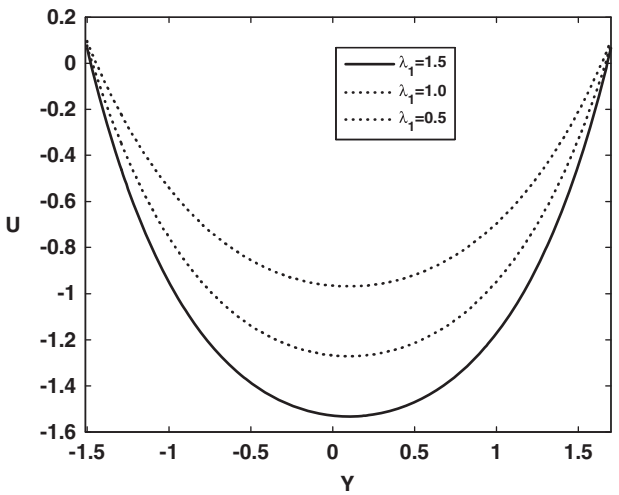

Figure 7. Velocity profile for different values of λ_1 at $a=0.7, b=1.2, d=1.5$, $X=1, t=1, q=-2, E=4, M=1, \phi=\pi/2, \beta=0.04$ (sinusoidal wave).

3. Trapezoidal wave:

$$h(x)=1+\phi\left[\frac{32}{\pi^2}\sum_{m=1}^{\infty}\frac{\sin\frac{\pi}{8}(2m-1)}{(2m-1)^2}\sin(2\pi(2m-1)x)\right]$$

DOI: 10.1002/fld

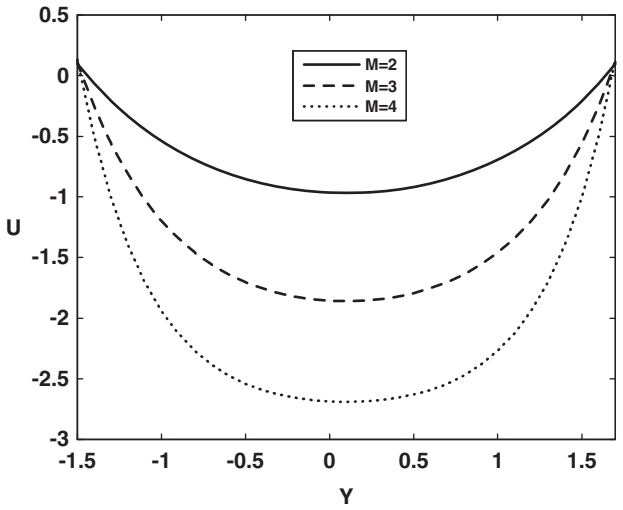

Figure 8. Velocity profile for different values of M at $a=0.7, b=1.2, d=1.5$, $X=1, t=1, q=-2, E=4, \lambda_1=0.5, \phi=\pi/2, \beta=0.04$ (sinusoidal wave).

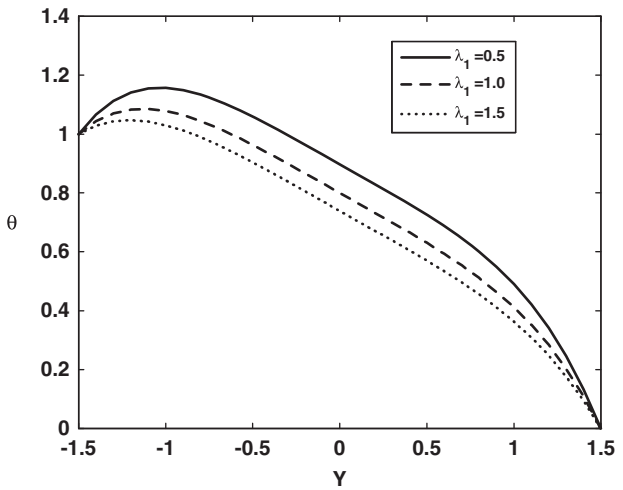

Figure 9. Variation of θ with Y for different values of λ_1 at $a=0.5, b=1.2, d=1.5$, $E=4, M=1, Pr=1, E_c=1, q=-0.1, \phi=\pi/2, \beta=0.04$ (sinusoidal wave).

5. GRAPHICAL RESULTS AND DISCUSSION

In this section, the graphical results are discussed to study the effects of various physical parameters on the pressure rise, frictional force, velocity, temperature, magnetic force function and stream lines. The expression for pressure rise and frictional force is calculated numerically using a mathematics

DOI: 10.1002/fld

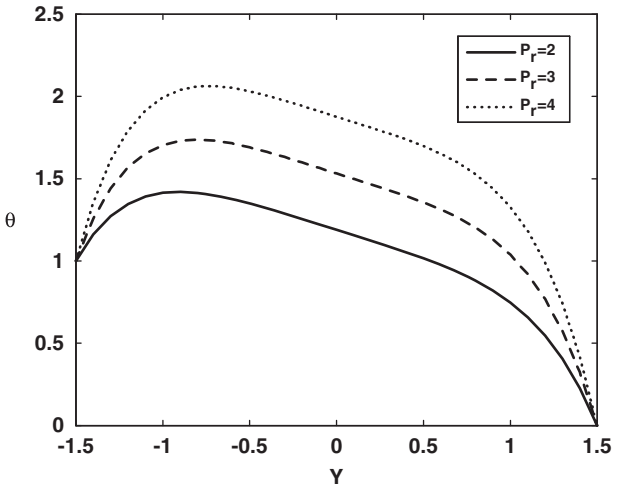

Figure 10. Variation of θ with Y for different values of Pr at $a=0.5, b=1.2, d=1.5, E=4$, $M=1, \lambda_1=0.4, q=-0.1, t=1, x=1, E_c=1, \phi=\pi/2, \beta=0.04$ (sinusoidal wave).

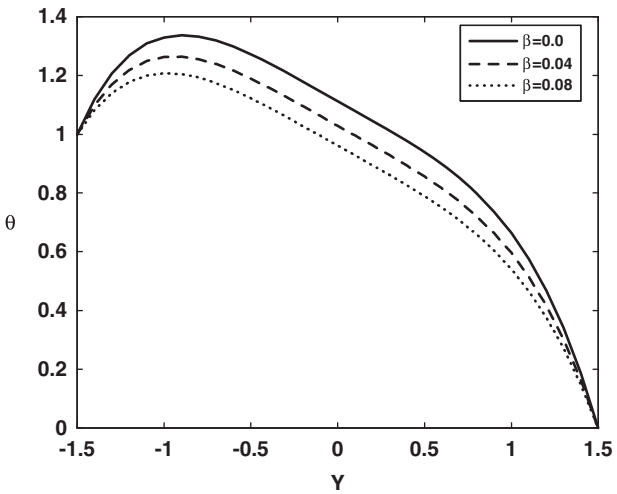

Figure 11. Variation of θ with Y for different values of β at $a=0.5, b=1.2, d=1.5, E=4$, $M=1, \lambda_1=0.4, q=-0.1, t=1, x=1, E_c=1, \phi=\pi/2, Pr=1$ (sinusoidal wave).

software. The graphical results of pressure rise, frictional force, velocity, magnetic force function and temperature are displayed in Figures 1–15. Figures 1–3 are prepared for pressure rise Δp against volume flow rate Q for different values of Jeffrey parameter λ_1, amplitude ratio ϕ and slip parameter β. It is observed that the relation between pressure rise and volume flow rate is inversely proportional to each other. It means that pressure rise gives larger values for small volume flow rate and it gives smaller values for large Q. Moreover, the peristaltic pumping occurs in

DOI: 10.1002/fld

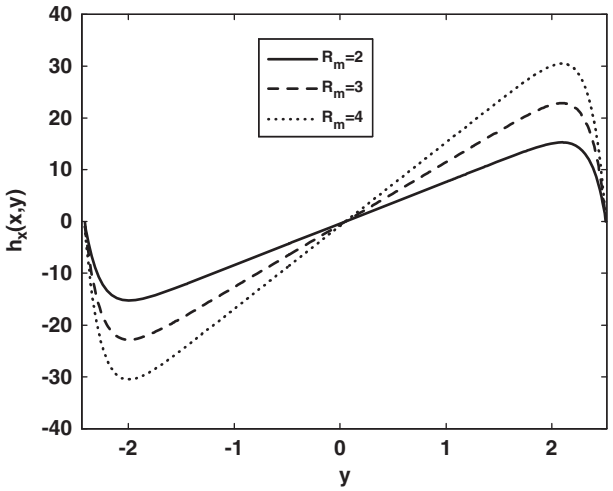

Figure 12. Variation of h_x with y for different values of R_{m} at $a=0.7, b=0.7, Q=-0.9$, $\beta=0.04, \phi=\pi, d=2.3, E=4, M=3, \lambda_1=4, x=0$ (sinusoidal wave).

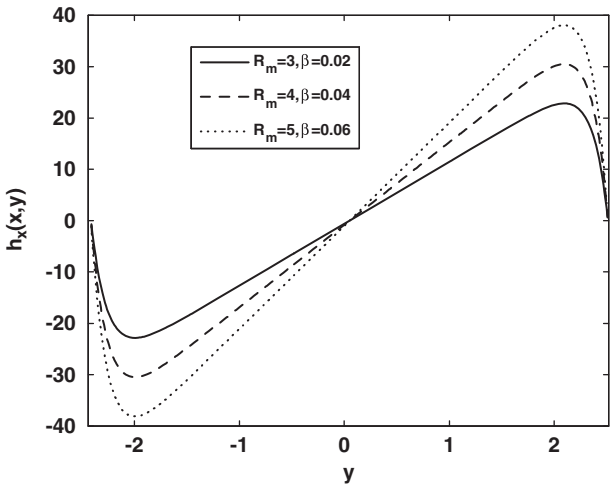

Figure 13. Variation of h_x with y for different values of R_{m} and β at $a=0.7, b=0.7$, $Q=-0.9, \phi=\pi, d=2.3, E=4, M=3, \lambda_1=4, x=0$ (sinusoidal wave).

the region $-1\leqslant Q<1.5$ for $\lambda_1, -1\leqslant Q\leqslant 1.7$ for ϕ and $-1\leqslant Q<1.5$ for β, otherwise augmented pumping occurs. The frictional forces F against flow rate Q for different values of λ_1, ϕ and β are shown in Figures 4–6. It is observed from the figures that frictional forces have opposite behavior as compared with the pressure rise. The velocity U for different values of λ_1 and M are shown in Figures 7 and 8. We observed that the velocity profile decreases with the decrease in λ_1 (see Figure 7). The effect of M on the velocity is almost opposite as compared with the

DOI: 10.1002/fld

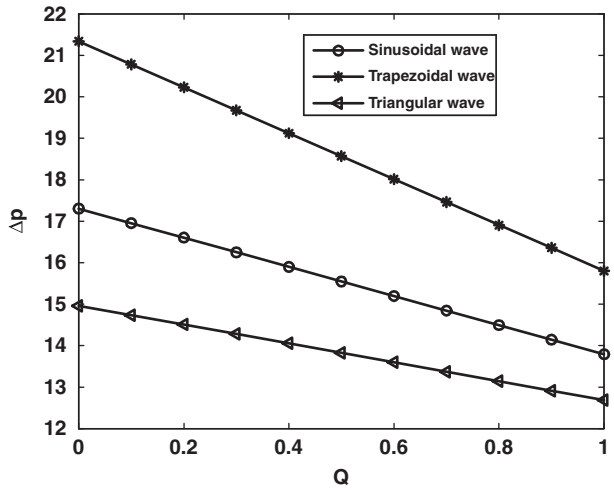

Figure 14. Variation of Δp with Q for different wave forms at $a=0.7$, $b=1.2, d=1.4, \phi=\pi, E=4, M=2, \lambda_1=0.8$.

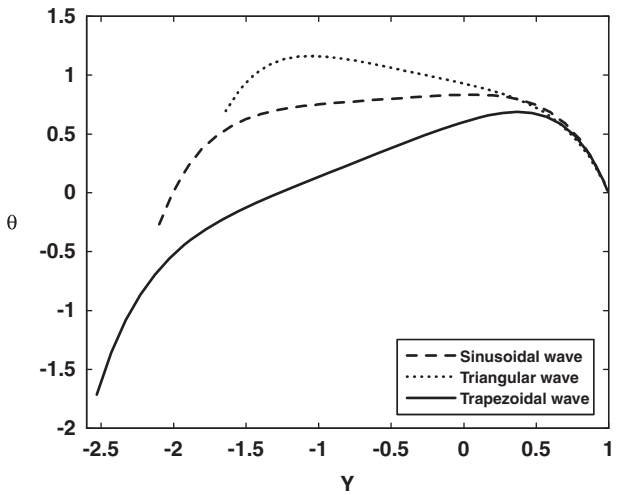

Figure 15. Variation of θ with Y for different wave forms at $a=0.5$, $b=1.2, d=1.5, \phi=\pi/6, E=4, E_c=1, Pr=1, M=1, \lambda_1=1, \beta=0.04$.

case of λ_1. Here, the velocity profile increases with the increase in M. The temperature fields for different values of λ_1, Pr and β against space variable Y are displayed in Figures 9–11. It is depicted that with the increase in λ_1 and β, the temperature field decreases while the temperature

DOI: 10.1002/fld

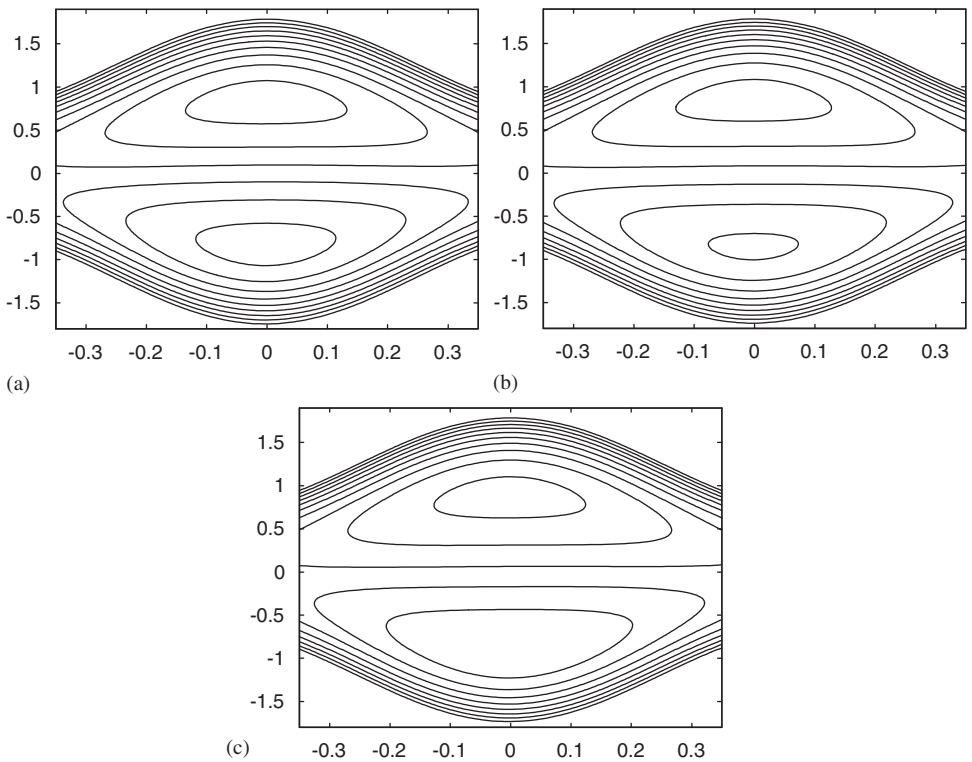

Figure 16. Stream lines for different values of λ_1: (a) for $\lambda_1 = 0.7$; (b) for $\lambda_1 = 0.8$; (c) for $\lambda_1 = 0.9$. The other parameters are $a = 0.5, b = 0.5, E = 1.5, M = 0.06, d = 1.0, \phi = 0.02, Q = 1.6$.

field increases with the increase in Pr. The expression for axial induced magnetic field h_x against space variable y for different values of magnetic Reynold number R_{m} and slip parameter β are shown in Figures 12–13. It is observed that with the increases in R_{m} and slip parameter β, h_x increases in the upper half of the channel while in the lower half the behavior is opposite.

The pressure rise for different kinds of wave shape are presented in Figure 14. It is observed that the pressure rise for sinusoidal wave is less than trapezoidal wave and greater than triangular wave. The temperature field θ for different wave shapes are shown in Figure 15. It is seen that the temperature field for triangular wave is greater than sinusoidal wave and sinusoidal wave is greater than trapezoidal wave.

The trapping phenomena for different values of λ_1, M and β are shown in Figures 16–19. It is observed from Figure 16 that the volume of the trapped bolus in the lower half channel is smaller as compared with the upper half of the channel. Moreover, the size of the trapped bolus decreases in the lower half of the channel with the increase in λ_1. It is depicted in Figure 17 that with the increase in M the size of the trapped bolus increases. The stream lines for different values of β are plotted in Figure 18. It is observed that the number and size of the trapped bolus decrease in the lower half of the channel and increase in the upper half of the channel with the increase in β. The stream lines for different wave shapes, such as sinusoidal wave, triangular wave and trapezoidal

DOI: 10.1002/fld

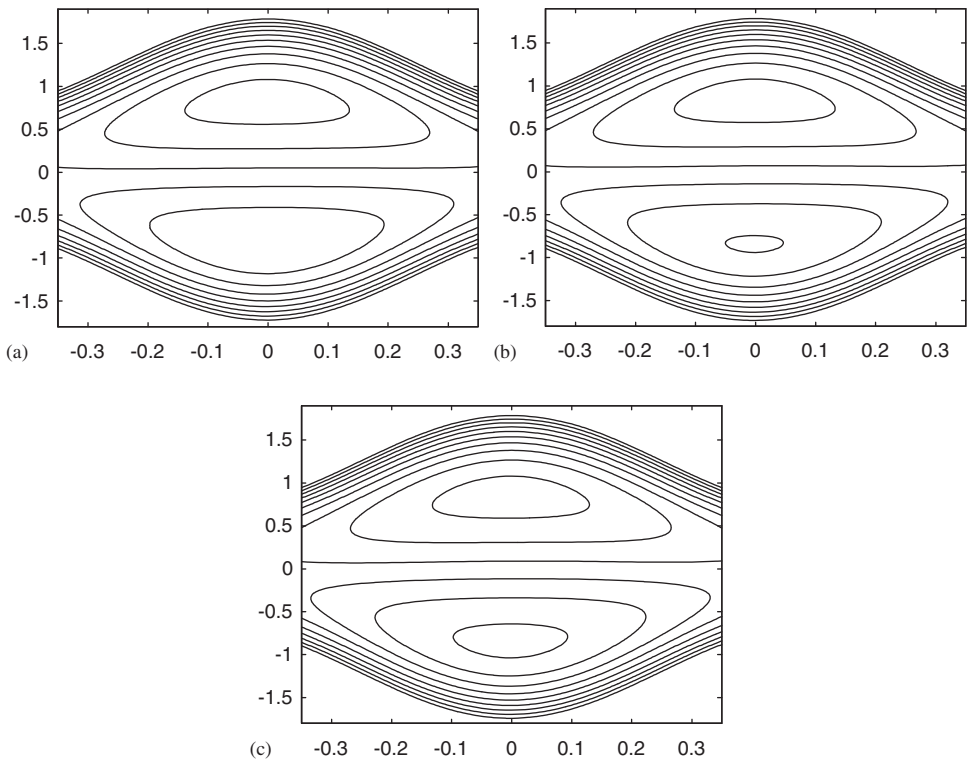

Figure 17. Stream lines for different values of M: (a) for $M=0.06$; (b) for $M=0.07$; (c) for $M=0.08$. The other parameters are $a=0.5, b=0.5, E=1.5, \lambda_1=0.8, \beta=0.01, d=1.0, \phi=0.02, Q=1.6$.

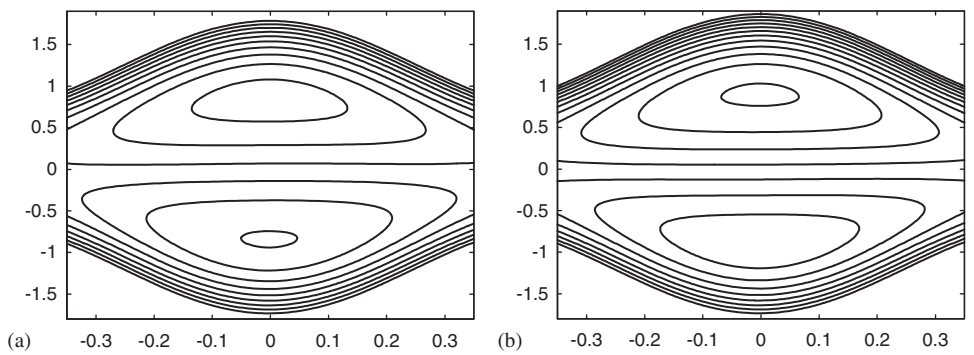

Figure 18. Stream lines for different values of β: (a) for $\beta=0.01$; (b) for $\beta=0.02$. The other parameters are $a=0.5, b=0.5, E=1.5, \lambda_1=0.8, d=1.0, \phi=0.02, Q=1.6$.

DOI: 10.1002/fld

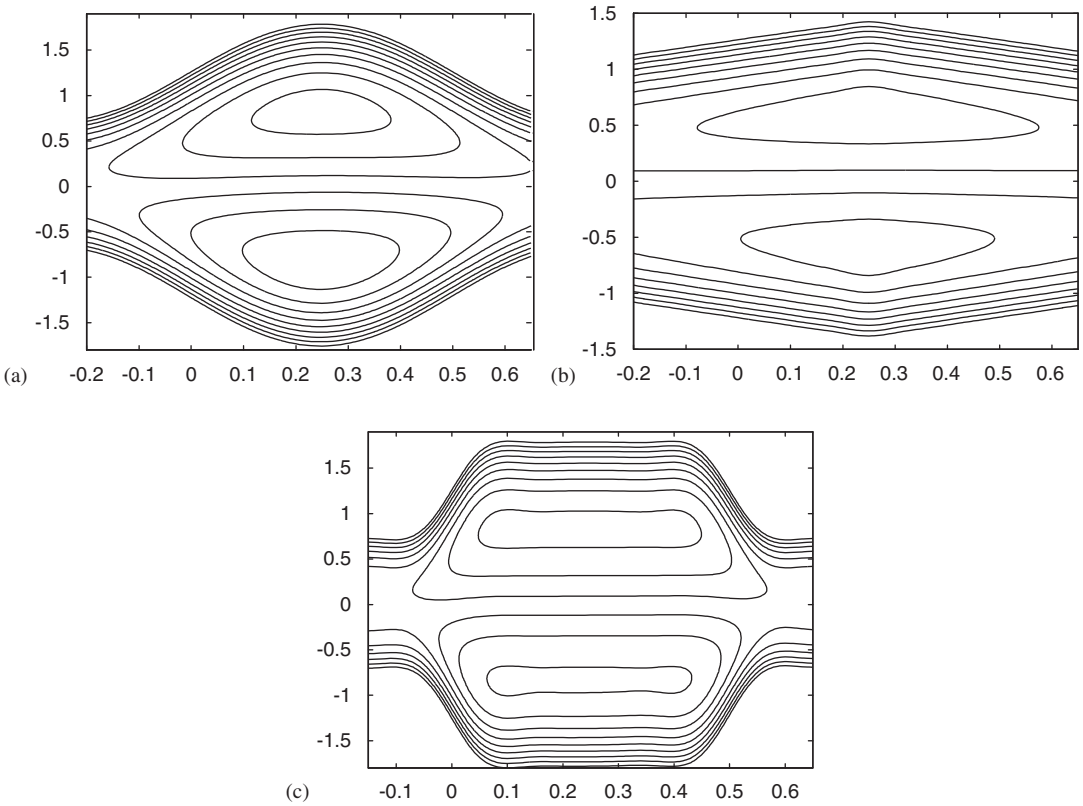

Figure 19. Stream lines for different wave forms (a) for sinusional wave; (b) for triangular wave; (c) for trapezoidal wave. The parameters are $a=0.5$, $b=0.5$, $E=1$, $\lambda_1=0.8$, $d=1.0$, $\phi=0.02$, $Q=1.6$, $\beta=0.01$.

Table I. Values of Nusselt number for different values of β (slip parameter), λ_1 (ratio of relaxation to retardation times), d (width of the channel) and Pr (Prandtl number). The other parameters are $a=0.5, b=1.2, E_c=1, x=1, t=1, M=1, \phi=\pi/2$.

β	Nu	λ_1	Nu	d	Nu	Pr	Nu
0.0	3.04216	0.0	3.77918	0.0	6.29996	0.0	0.333333
0.01	2.95211	0.2	3.25119	0.2	3.44381	0.4	0.839961
0.02	2.86647	0.4	2.86647	0.4	2.86647	0.8	1.34659
0.03	2.78497	0.6	2.57392	0.6	2.49755	1.2	1.85322
0.04	2.70733	0.8	2.34411	0.8	2.17929	1.6	2.35984
0.05	2.6333	1.0	2.15892	1.0	1.9118	2.0	2.86647

wave, are shown in Figure 19. The behavior of Nusselt number for different values of physical parameters is shown in Table I. The table shows that with the increase in β, λ_1, and d, the Nusselt number decreases while with the increase in prandtl number, Pr, the Nusselt number increases.

DOI: 10.1002/fld

REFERENCES

1. Beavers GS, Joseph DD. Boundary conditions at a naturally permeable wall. *Journal of Fluid Mechanics* 1967; **30**:197–207.
2. Laplace P, Arquis E. Boundary layer over a slotted plate. *European Journal of Fluid Mechanics B/Fluids* 1998; **17**:331–355.
3. Miksis MJ, Davis SH. Slip over rough and coated surface. *Journal of Fluid Mechanics* 1994; **273**:125–139.
4. Gad-el-Hak M. The fluid mechanics of microdevices—The Freeman scholar lecture. *ASME Journal of Fluids Engineering* 1999; **121**:5–33.
5. Navier CLM. Sur les lois du mouvement des fluids. Comptef Rendus des Seances de l. *Academie des Sciences* 1827; **6**:389–440.
6. Sajid M, Awais M, Nadeem S, Hayat T. The influence of slip condition on thin film flow of a fourth grade fluid by the homotopy analysis method. *Computers and Mathematics with Applications* 2008; **56**:2019–2026.
7. Hayat T, Javed T, Abbas Z. Slip flow and heat transfer of a second grade fluid past a stretching sheet through a porous space. *International Journal of Heat and Mass Transfer* 2008; **51**:4528–4534.
8. Donald Ariel P. Axisymmetric flow due to a stretching sheet with partial slip. *Computers and Mathematics with Applications* 2007; **54**:1169–1183.
9. Hayat T, Hussain Q, Ali N. Influence of partial slip on the peristaltic flow in a porous medium. *Physica A* 2008; **387**:3399–3409.
10. Eldabe NT, Elghazy EM, Ebaid A. Closed form solution to a second order boundary value problem and its application in fluid mechanics. *Physics Letters A* 2007; **363**:257–259.
11. Mekheimer KhS, ElShehawey EF, Alaw AM. Peristaltic motion of a particle fluid suspension in a planar channel. *International Journal of Theoretical Physics* 1998; **37**:2895–2920.
12. Mishra M, Rao AR. Peristaltic transport of a Newtonian fluid in an asymmetric channel. *Zeitschrift fur Angewandte Mathematik and Physik* 2004; **54**:532–550.
13. Misery AEM, El Shehawey EF, Hakeem AA. Peristaltic motion of an incompressible generalized Newtonian fluid in a planar channel. *Journal of Physical Society of Japan* 1996; **65**:3524–3529.
14. Shapiro AH, Jaffrin MY, Weinberg SL. Peristaltic pumping with long wave length at low Reynolds number. *Journal of Fluid Mechanics* 1969; **37**:799–825.
15. Hayat T, Ali N, Abbas Z. Peristaltic flow of a micropolar fluid in a channel with different wave forms. *Physics Letters A* 2007; **370**:331–344.
16. Haroun MH. Effect of Deborah number and phase difference on peristaltic transport in an asymmetric channel. *Communications in Nonlinear Science and Numerical Simulation* 2007; **12**:1464–1480.
17. Haroun MH. Non-linear peristaltic flow of a fourth grade fluid in an inclined asymmetric channel. *Computer and Material Sciences* 2007; **39**:324–333.
18. Kotkandapani M, Srinivas S. Non-linear peristaltic transport of Newtonian fluid in an inclined asymmetric channel through a porous medium. *Physics Letters A* 2008; **372**:1265–1276.
19. Mekheimer KhS, Abd elmaboud Y. The influence of heat transfer and magnetic field on peristaltic transport of a Newtonian fluid in a vertical annulus: an application of an endoscope. *Physics Letters A* 2008; **372**:1657–1665.
20. Wang Y, Hayat T, Hutter K. On non-linear magnetohydrodynamics problems of an Oldroyd-6-constant fluid. *International Journal of Non-linear Mechanics* 2005; **40**:40–58.
21. Hayat T, Ali N. Peristaltically induced motion of a MHD third grade fluid in a deformable tube. *Physica A* 2006; **370**:225–239.
22. Hayat T, Ahmad Niaz, Ali N. Effects of an endoscope and magnetic field on the peristalsis involving Jeffrey fluid. *Communications in Nonlinear Science and Numerical Simulation* 2008; **13**:1581–1591.
23. Mekheimer KhS. Effect of the induced magnetic field on peristaltic flow of a couple stress fluid. *Physics Letters A* 2008; **372**:4271–4278.
24. Elshehawey EF, Eladabe NT, Elghazy EM, Ebaid A. Peristaltic transport in an asymmetric channel through a porous medium. *Applied Mathematics and Computation* 2006; **182**:140–150.
25. Nadeem S, Noreen SA. Effects of heat transfer on the peristaltic transport of MHD Newtonian fluid with variable viscosity: application of Adomian decomposition method. *Communications in Nonlinear Science and Numerical Simulation*. DOI: 10.1016/j.cnsns.2008.09.010.
26. Mekheimer KhS. Effect of the induced magnetic field on peristaltic flow of a couple stress fluid. *Physics Letters A* 2008; **372**:4271–4278.
27. Srivastava LM, Agrawal RP. Oscillating flow of a conducting fluid with suspension of spherical particles. *Journal of Applied Mechanics* 1980; **47**:196–199.